

X-ray emission from dark clusters of MACHOs

F. De Paolis¹, G. Ingrosso², Ph. Jetzer¹, and M. Roncadelli³

¹ Paul Scherrer Institute, Laboratory for Astrophysics, CH-5232 Villigen PSI, and Institute of Theoretical Physics, University of Zurich, Winterthurerstrasse 190, CH-8057 Zurich, Switzerland

² Dipartimento di Fisica, Università di Lecce, and INFN, Sezione di Lecce, Via Arnesano, CP 193, I-73100 Lecce, Italy

³ INFN, Sezione di Pavia, Via Bassi 6, I-27100, Pavia, Italy

Received date; accepted date

Abstract. MACHOs (Massive Astrophysical Compact Halo Objects) - as discovered by microlensing experiments towards the LMC - provide a natural explanation for the galactic halo dark matter. A realistic possibility is that MACHOs are brown dwarfs of mass $\sim 0.1 M_{\odot}$. Various arguments suggest that brown dwarfs should have a coronal X-ray emission of $\sim 10^{27}$ erg s⁻¹. As MACHOs are presumably clumped into dark clusters (DCs), each DC is expected to have a total X-ray luminosity of $\sim 10^{29} - 10^{32}$ erg s⁻¹. We discuss the possibility that dark clusters contribute to the diffuse X-ray background (XRB) or show up as discrete sources in very deep field X-ray satellite observations. Moreover, from the observed diffuse XRB we infer that the amount of virialized diffuse gas present in the galactic halo can at most make up 5% of the halo dark matter.

Key words: Dark matter - The halo of the Galaxy - Dwarf stars - X-rays: general

1. Introduction

In spite of the dynamical evidence that a lot of dark matter is concealed in galactic halos, observations failed for many years to provide any information about its nature. A breakthrough came recently with the discovery of Massive Astrophysical Compact Halo Objects (MACHOs) in microlensing experiments towards the Large Magellanic Cloud (Alcock et al. 1993; Aubourg et al. 1993). Today, although the existence of MACHOs - presumably located in the halo of our galaxy - appears to be firmly established, the implications of such an achievement are still largely unsettled, owing to their sensitive dependence on the assumed galactic model (Gates, Gyuk & Turner 1996). More specifically, the existing data-set permits to reliably conclude that MACHOs should lie in the mass range $0.05 M_{\odot} - 1.0 M_{\odot}$, but stronger claims are unwarranted because the inferred MACHO mass strongly depends on the uncertain properties of the considered galactic model (Evans 1996, De Paolis, Ingrosso & Jetzer 1996).

Even if present uncertainties do not yet permit to make any sharp statement about the nature of MACHOs, brown dwarfs

look as a viable possibility to date, and we shall stick to it throughout.

Remarkably enough, a simple scenario has been proposed (De Paolis et al. 1995; Gerhard & Silk 1996; Nulsen and Fabian 1997) which - besides encompassing the Fall-Rees theory for the formation of globular clusters (Fall & Rees 1985) - predicts that dark clusters of brown dwarfs and cold molecular clouds (mainly of H_2) should form in the halo at galactocentric distances larger than 10-20 kpc. Dark clusters in the mass range $3 \times 10^2 - 10^6 M_{\odot}$ are expected to have survived all disruptive effects and should still populate the outer galactic halo today (De Paolis et al. 1996a, 1996b).

In this paper we would like to discuss further aspects of the above scenario, which naturally arise provided MACHOs have coronal X-ray emission. Indeed, X-ray observations of field stars have shown that low-mass stars - with mass even as low as $0.08 M_{\odot}$ - do have coronal X-ray emission. Thus - given that MACHOs are old, very low-mass stars - we expect them to be X-ray active. Actually, under this assumption, Kashyap et al. 1994 have explored the possibility that an *unclustered* MACHO population in the galactic halo can contribute significantly (at levels $> 10\%$) to the diffuse X-Ray Background (XRB) at higher (≥ 0.5 keV) energies. As we shall see in Sect. 4, such an unclustered distribution looks however unpalatable. Apart from automatically avoiding this difficulty, the scenario under consideration has two further implications as far as X-ray emission is concerned. First, the gas present in the DCs partially shields the X-ray emission from MACHOs, thereby reducing the total contribution to the XRB (as compared with the expectation of Kashyap et al. 1994). Second - besides contributing to the diffuse XRB - DCs can also show up as discrete sources in analyses of very deep field X-ray satellite observations towards regions in the sky of very low column density.

In fact, the existence of a new population of not yet fully recognized X-ray sources has been suggested by an analysis of very deep ROSAT observations (towards the *Lockman Hole*), which revealed a considerable excess of faint X-ray sources over that expected by Active Galactic Nuclei (AGN) evolution models (Hasinger et al. 1993). A re-analysis of the same data shows that most of the sources in excess may be identified with clusters of galaxies and narrow emission or absorption line galaxies (Hasinger 1996). Recently, data analyses of ROSAT observations in a different region of the sky (McHardy et al. 1997) have confirmed the previous conclusions by Hasinger 1996 and

Send offprint requests to: Ph. Jetzer

make even more clear that below a flux level of $\sim 3 \times 10^{-15}$ erg cm $^{-2}$ s $^{-1}$ there exists a population of unidentified, faint point-like X-ray sources (about 10-20% of the total). Still, an open problem is whether the unidentified sources are galactic or extragalactic in origin. Our main point is that a galactic population of DCs can significantly contribute to the inferred new population in question.

The plan of the paper is as follows. In Section 2 we discuss the questions concerning the DCs X-ray emission, while the observational implications of the scenario under consideration are addressed in Section 3. Limits on the amount of the virialized X-ray emitting diffuse gas in the galactic halo are derived in Section 4. Our conclusions are summarized in Section 5.

2. Dark Clusters and X-ray Emission

As is well known, low-mass stars have coronal X-ray emission due to the presence of collisionally excited plasma in their convective envelopes. Observations have shown that the coronal gas temperature T lies in the range $\sim 10^6 - 10^8$ K (Schmitt et al. 1990). As regard to the corresponding X-ray luminosity, measurements performed by EINSTEIN and ROSAT satellites yield the average value $L_X \sim 10^{27}$ erg s $^{-1}$ for late M-stars (Barbera et al. 1993, Fleming et al. 1993). Moreover, neither any obvious correlation between L_X and bolometric luminosities for K and M-stars has been found (Mullan and Fleming 1996), nor a dependence of L_X on the metallicity has been detected (Kashyap et al. 1994). Now, brown dwarfs are very low-mass stars which share several features in many spectral bands with late M-stars. So, it seems plausible to expect MACHOs to have coronal X-ray emission as well¹. More specifically, we assume that MACHOs have an average X-ray luminosity $L_X^M \sim 10^{27}$ erg s $^{-1}$ in the 0.1 – 10 keV energy band. Our attitude is further supported by the direct observation of at least one object, the VB 8 dwarf (of mass $\simeq 0.08 M_\odot$), by EINSTEIN, EXOSAT and ROSAT satellites between 1979 and 1994, whose measured X-ray luminosity is 1.8×10^{28} erg s $^{-1}$, 2.6×10^{27} erg s $^{-1}$ and 8.3×10^{26} erg s $^{-1}$ in the energy bands 0.05 – 2 keV, 0.12 – 3.7 keV and 0.1 – 2.4 keV, respectively (Drake et al. 1996).

Let us focus our attention on the coronal plasma emissivity $\epsilon_\nu(\nu, T, Z) = f(\nu, T, Z) n_i n_e$, where Z denotes the gas metallicity, n_i and n_e are the ion and electron number density, respectively (we shall use cgs units throughout the paper). Following Raymond and Smith 1977, this quantity is obtained by adding the continuum energy emissivity (by free-free and free-bound processes) to the emission-line contribution by metals (through bound-bound processes). We may confidently suppose that the primordial halo gas from which MACHOs have formed has a metallicity $Z \sim 10^{-2} Z_\odot$ (from now on - with the exception of Section 4 - this value will be implicitly assumed throughout and the Z -dependence in the ensuing expressions will be dropped). Hence, the X-ray spectral luminosity $L_\nu^M(\nu, T)$ of a single MACHO is obtained by integrating ϵ_ν over the coronal volume V_c . However, in the present instance, we do not need to know V_c , n_i and n_e due to the obvious requirement that integration of $L_\nu^M(\nu, T)$ over the frequency range $0.1 \text{ keV}/h \leq \nu \leq 10 \text{ keV}/h$ is equal to the total X-ray MACHO luminosity L_X^M . In this way, we find

¹The X-ray emission from lower mass objects (such as Jupiter-sized planets) is ignorable for our purposes, owing to their low X-ray luminosity $\sim 10^{16} - 10^{17}$ erg s $^{-1}$.

$$L_\nu^M(\nu, T) = \frac{f(\nu, T)}{\int_{0.1 \text{ keV}/h}^{10 \text{ keV}/h} d\nu f(\nu, T)} L_X^M. \quad (1)$$

Next, we compute the X-ray luminosity $\mathcal{L}_X^{DC}(\nu_1, \nu_2)$ of a DC in the frequency range (ν_1, ν_2) taking the X-rays absorption by molecular clouds within the DC into account (absorption by the galactic disk is momentarily disregarded). To this end, it is convenient to consider first the X-ray luminosity $I_X(b, \nu_1, \nu_2)$ in the frequency range (ν_1, ν_2) from a unit element of the DC projected surface – perpendicular to the line of sight – at impact parameter b . We denote by y the coordinate along the line of sight (with origin on the perpendicular plane through the centre of the DC), and by n_M and n_{mol} the number density of MACHOs and gas, respectively, in a DC. In addition, $\sigma_X(\nu)$ stands for the X-ray absorption cross-section whereas R_{DC} denotes the (median) radius of a DC. It follows that the optical depth inside a DC is

$$\tau_{DC}(\nu, b, y) = \int_y^{\sqrt{R_{DC}^2 - b^2}} dy' \sigma_X(\nu) n_{\text{mol}}. \quad (2)$$

Moreover, a straightforward calculation yields

$$I_X(b, \nu_1, \nu_2) = \int_{\nu_1}^{\nu_2} d\nu \times \int_{-\sqrt{R_{DC}^2 - b^2}}^{\sqrt{R_{DC}^2 - b^2}} dy n_M L_\nu^M(\nu, T) e^{-\tau_{DC}(\nu, b, y)}. \quad (3)$$

Because of the spherical symmetry, we ultimately get

$$\mathcal{L}_X^{DC}(\nu_1, \nu_2) = \int_0^{R_{DC}} I_X(b, \nu_1, \nu_2) 2\pi b db. \quad (4)$$

What are n_M and n_{mol} ? Although the gas distribution is expected to be clumpy, for simplicity we can safely adopt a uniform average distribution, so that n_{mol} is constant. As discussed elsewhere (De Paolis et al. 1996a, 1996b), in the lack of any observational information about DCs it seems natural to take their average mass density equal to that of globular clusters. Then the following relationship ensues $R_{DC} = 0.12 (M_{DC}/M_\odot)^{1/3}$ (M_{DC} is the mass of a DC). On account of it, n_{mol} becomes independent of M_{DC} and R_{DC} , and its explicit value is $\sim 10^3$ cm $^{-3}$. The case of n_M is less trivial, since the results we are going to derive can depend strongly on how MACHOs are distributed inside DCs. Below, we consider the two extreme situations: (a) all MACHOs are uniformly distributed in the DCs; (b) all MACHOs are concentrated in the DC cores. Realistically, we expect an intermediate situation to occur, since the mass stratification instability drives the more massive MACHOs into the cluster cores. In addition, DCs with mass in the range $3 \times 10^2 M_\odot \lesssim M_{DC} \lesssim 5 \times 10^4 M_\odot$ should have started core collapse (De Paolis et al. 1996b), in which case situation (b) becomes an excellent approximation.

Let us proceed to address the two cases separately. In case (a), $I_X(b, \nu_1, \nu_2)$ can be computed analytically to give

$$I_X(b, \nu_1, \nu_2) = \frac{n_M}{n_{\text{mol}}} \int_{\nu_1}^{\nu_2} d\nu L_\nu^M(\nu, T) \times \frac{1 - e^{-2\sigma_X(\nu) n_{\text{mol}} \sqrt{R^2 - b^2}}}{\sigma_X(\nu)}. \quad (5)$$

By inserting expression (5) into equation (4) we obtain

$$\mathcal{L}_X^{DC}(\nu_1, \nu_2) = 10f \left(\frac{M_{DC}}{M_\odot} \right) L_X^M g(\nu_1, \nu_2, T), \quad (6)$$

where f is the fraction of DC matter in the form of MACHOs, $\beta \equiv \tau_{DC}(\nu, 0, 0)$ and we have introduced the attenuation factor

$$g(\nu_1, \nu_2, T) = \int_{\nu_1}^{\nu_2} \frac{3L_\nu^M(\nu, T)}{4L_X^M} \left[\frac{1}{\beta} + \frac{e^{-2\beta}}{\beta^2} + \frac{e^{-2\beta} - 1}{2\beta^3} \right] d\nu \quad (7)$$

which yields the fraction of X-rays emerging from a DC. Case (b) can be handled in a similar fashion with eq. (7) replaced by

$$g(\nu_1, \nu_2, T) = \int_{\nu_1}^{\nu_2} d\nu \frac{L_\nu^M(\nu, T)}{L_X^M} e^{-\beta}. \quad (8)$$

What about $\sigma_X(E)$? It is well known that for X-rays incoming on gas with interstellar composition $\sigma_X(E) \simeq 2.6 \times 10^{-22} E^{-8/3} \text{ cm}^{-2}$ with E in keV (Morrison and McCammon 1983). On the other hand, in the limiting case of $Z = 0$ it turns out that $\sigma_X(E) \simeq 4 \times 10^{-24} E^{-3} \text{ cm}^{-2}$ (see Fig. 1 in Morrison and McCammon 1983). Since we are dealing with the case $Z \sim 10^{-2} Z_\odot$, we shall use for $\sigma_X(E)$ in eq. (5) the linear interpolation between the above expressions.

We report in Table 1 the values of $g(\nu_1, \nu_2, T)$ for various energy bands and different values of the MACHO coronal gas temperature T in both cases (a) and (b). As we can see, the fraction of X-rays surviving the absorption by molecular clouds in DCs ranges from $\sim 0.1\%$ to $\sim 74\%$.

Table 1. The attenuation function g - see eqs. (7)-(8) - is displayed for selected values of the MACHO coronal temperature T in different energy bands (the first and second ones are the ROSAT medium and high-energy bands while the third refers to the EPIC instrument on the planned satellite XMM). We consider two cases: (a) MACHOs uniformly distributed in the DCs and (b) MACHOs concentrated in the DC cores. For the latter case, we give in the last column the X-ray flux Φ_X^{DC} - see eq.(9) - reaching the Earth, assuming, as an illustration, $f = 1/2$, $r = 20 \text{ kpc}$, $M_{DC} = 10^5 M_\odot$ and $L_X^M = 10^{27} \text{ erg s}^{-1}$. We have verified that in the low ROSAT energy band 0.15-0.28 keV the X-ray absorption is so efficient that we cannot hope to detect any radiation coming from a DC.

| $E_1 - E_2$ (keV) | T (K) | $g(\nu_1, \nu_2, T)$ | $g(\nu_1, \nu_2, T)$ | Φ_X^{DC} (erg cm ⁻² s ⁻¹) |
|----------------------|-----------------|----------------------|----------------------|--|
| | | case (a) | case (b) | case (b) |
| 0.5 – 0.9 | 10 ⁶ | 4.4×10^{-3} | 5.6×10^{-4} | 5.8×10^{-18} |
| | 10 ⁷ | 5.7×10^{-2} | 1.8×10^{-2} | 1.8×10^{-16} |
| | 10 ⁸ | 2.1×10^{-2} | 6.6×10^{-3} | 6.8×10^{-17} |
| 0.1 – 2.5 | 10 ⁶ | 1.7×10^{-2} | 8.5×10^{-4} | 8.8×10^{-18} |
| | 10 ⁷ | 3.0×10^{-1} | 2.2×10^{-1} | 2.3×10^{-15} |
| | 10 ⁸ | 2.3×10^{-1} | 1.9×10^{-1} | 2.0×10^{-15} |
| 0.1 – 10 | 10 ⁶ | 1.5×10^{-1} | 8.5×10^{-3} | 8.6×10^{-17} |
| | 10 ⁷ | 3.7×10^{-1} | 2.6×10^{-1} | 2.7×10^{-15} |
| | 10 ⁸ | 7.4×10^{-1} | 6.9×10^{-1} | 7.3×10^{-15} |

At this point, we take into account the absorption by the galactic disk. Actually, the foregoing analysis can be easily extended to this case by replacing $\tau_{DC}(\nu, b, y)$ with $\tau_{DC}(\nu, b, y) + \tau_{\text{disk}}(\nu)$. Although the latter quantity depends on the galactic coordinates, for simplicity we take the average value $\tau_{\text{disk}}(\nu) \simeq 6 \times 10^{19} \sigma_X(\nu) \text{ cm}^{-2}$,² and so the flux from a single DC at distance r from Earth is

$$\Phi_X^{DC}(\nu_1, \nu_2) = 0.8 \frac{f}{r^2} \left(\frac{M_{DC}}{M_\odot} \right) L_X^M g(\nu_1, \nu_2, T). \quad (9)$$

Values of $\Phi_X^{DC}(\nu_1, \nu_2)$ are reported in Table 1, for the typical situation $r = 20 \text{ kpc}$, $M_{DC} = 10^5 M_\odot$, $f = 0.5$ and $L_X^M = 10^{27} \text{ erg s}^{-1}$. Of course, this is only an illustrative case, since we expect $3 \times 10^2 M_\odot \lesssim M_{DC} \lesssim 10^6 M_\odot$ and $r \gtrsim 10 - 20 \text{ kpc}$.

Let us now estimate the number \mathcal{N} of DCs within a square degree in the sky. Taking indicatively $\sim 10^{12} M_\odot$ for the mass of the dark halo of our galaxy (Zaritsky 1989), we get $\mathcal{N} \simeq 2.4 \times 10^7 (M_\odot/M_{DC}) \text{ deg}^{-2}$. Thus, for $3 \times 10^2 M_\odot \lesssim M_{DC} \lesssim 10^6 M_\odot$, we expect \mathcal{N} in the range $24 - 80,000 \text{ deg}^{-2}$. On the other hand, the angular size of a DC at distance r from Earth is $\theta \simeq 0.4' (M_{DC}/M_\odot)^{1/3} (\text{kpc}/r)$, and so we get $2.7' (\text{kpc}/r) \lesssim \theta \lesssim 40' (\text{kpc}/r)$ for M_{DC} in the above range. However, it is crucial to stress that the effective angular size of DCs in the X-ray band can be much smaller than that. Indeed, the DCs with $3 \times 10^2 M_\odot \lesssim M_{DC} \lesssim 5 \times 10^4 M_\odot$ should have started core collapse, and so MACHOs are expected to be concentrated towards the centre.

An important issue concerns the spectrum of X-rays surviving absorption by molecular clouds and thereby emerging from a DC. The energy-dependence of $\sigma_X(E)$ implies (due to the more efficient X-ray absorption at low-energy) a hardening of the X-ray spectrum. In order to quantify this effect, it is useful to define the hardness ratio $HR = (H - S)/(H + S)$ as in Hasinger et al. 1993, where H and S are the fluxes in the 0.1–0.4 and 0.4–2.4 keV bands, respectively. It turns out that absorption substantially increases the hardness ratio, leading to $HR \sim 1$.

3. Observational implications

We turn now our attention to the observational implications of the above analysis. Various parameters – namely f , M_{DC} , T and L_X^M – play a key-rôle in the present considerations. Unfortunately, they are poorly constrained from a theoretical point of view. Therefore, only by explicitly resorting to the experimental setup can we figure out under what conditions DCs are observable in the X-ray band. In order to make our discussion more definite, we shall henceforth consider the typical situation in which $f \simeq 0.5$, $T \simeq 10^7 \text{ K}$ and $L_X^M \simeq 10^{27} \text{ erg s}^{-1}$, whereas M_{DC} will be left as a free parameter in the above-considered range (however, the results corresponding to $T \simeq 10^6 \text{ K}$ and $T \simeq 10^8 \text{ K}$ are exhibited in Table 1 and Fig. 2). It should be pointed out that it still remains to be decided between cases (a) and (b) discussed in Section 2. As it can be seen from Table 1, the difference turns out to be very small, and since realistically we expect an intermediate situation to occur, we take for $g(\nu_1, \nu_2, T)$ the average value.

²We use this value, which is slightly less than the usual one, since we are mainly interested in observations towards regions of very low HI column density.

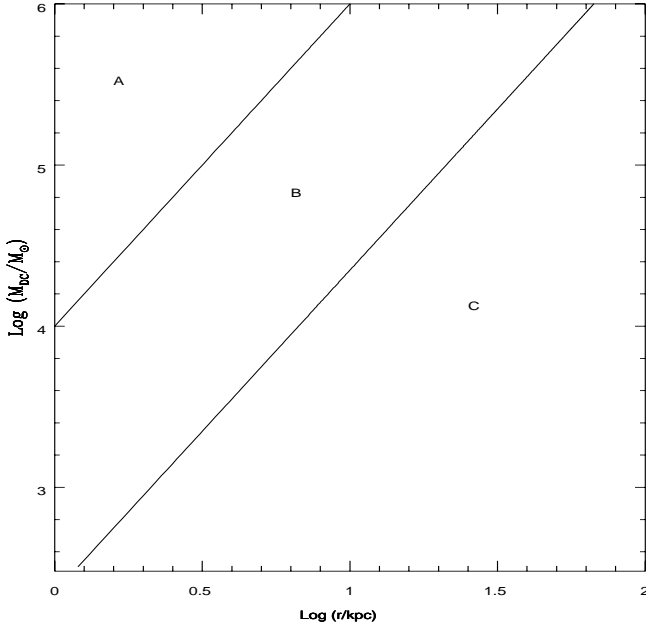


Fig. 1. It is shown how the plane $M_{DC} - r$ gets divided into three regions depending on different observational expectations. Assuming a disk gas column density of $6 \times 10^{19} \text{ cm}^{-2}$ (the same as towards the *Lockman Hole*), DCs in region A are observable as resolved sources. DCs in region B are to show up as background fluctuations in deep-field exposures. DCs in region C can only contribute to the diffuse XRB.

Presently, ROSAT is by far the most sensitive X-ray telescope in the $0.1 - 2.5 \text{ keV}$ energy range, and so the subsequent analysis will rest upon its instrumental capabilities. Its sensitivity threshold for detecting DCs as resolved sources in medium-exposures is $\simeq 10^{-13} \text{ erg cm}^{-2} \text{ s}^{-1}$, whereas a statistical analysis of the *background fluctuations* in deep-exposures can be carried out down to $\simeq 2.5 \times 10^{-15} \text{ erg cm}^{-2} \text{ s}^{-1}$ (Hasinger et al. 1993). Combining these sensitivity thresholds with eq. (9), we single out the various observational prospects for the DCs. More specifically (as it is shown in Fig. 1), the $r - M_{DC}$ parameter plane gets divided into three regions A, B and C (notice that we also take into account the constraint $3 \times 10^2 M_{\odot} \lesssim M_{DC} \lesssim 10^6 M_{\odot}$). Region A comprises DCs which are observable as resolved sources – this region turns out to be severely constrained by ROSAT data. DCs in region B are to show up as background fluctuations in deep-field exposures. Finally, DCs in region C are too faint to be detected nowadays and would, therefore, merely contribute to the diffuse XRB.

3.1. Dark clusters as resolved objects

Let us first address the possibility of detecting DCs as resolved (discrete) sources. Inspection of eq. (9) and Table 1 shows that the chance is presently rather dim. However, a considerable improvement is offered by the next-generation of satellite-borne X-ray detectors (like XMM), whose sensitivity is expected to be at least one order of magnitude better than for ROSAT. Then the more massive DCs (with $M_{DC} \sim 10^6 M_{\odot}$) should be observed as resolved sources. Moreover, it seems to us that the most promising strategy should be to look towards a previously microlensed star in the LMC.

3.2. Dark clusters and the new population of faint X-ray sources

Next, we proceed to discuss whether DCs form a new population of faint X-ray sources. Actually, fluctuation analyses of the XRB in the direction of the *Lockman Hole* (with the lowest *HI* column density) have led to the discovery of $\simeq 120 \text{ deg}^{-2}$ unidentified discrete sources in the $0.5 - 2 \text{ keV}$ energy band with flux in the range $2.5 \times 10^{-15} - 10^{-13} \text{ erg cm}^{-2} \text{ s}^{-1}$ over the extrapolation from AGN evolution models (Hasinger et al. 1993). As pointed out by these authors, one way to solve this discrepancy could be to adopt different parameters or more complicated evolutionary models for AGNs. Another explanation would be the existence of a new population of faint X-ray sources, which cannot be identified with any class of known objects (as stars, BL Lac objects, clusters of galaxies and normal galaxies). A re-analysis of the same data (Hasinger 1996) shows that most of these sources in excess (with respect to AGNs) may be identified with clusters of galaxies and narrow emission or absorption line galaxies. Similar results have been obtained by analyses (down to a flux limit of $1.6 \times 10^{-15} \text{ erg cm}^{-2} \text{ s}^{-1}$) of ROSAT observations towards a different region in the sky with the deepest optically identified X-ray survey made so far (McHardy et al. 1997). These observations further support the existence of an unidentified population of faint (with flux $< 3 \times 10^{-15} \text{ erg cm}^{-2} \text{ s}^{-1}$), point-like (namely with angular size less than the instrumental resolution $\sim 20''$) X-ray sources.

What is not clear at the moment is whether these sources are galactic or extragalactic in origin. Maoz and Grindlay 1995 have argued that the new population is wholly galactic.

Our main point is that DCs can contribute to this new population of faint X-ray sources (of course, we are supposing that MACHOs are concentrated inside the DC cores). To this end, we have to compute the number \mathcal{N} of DCs per square degree with flux above $2.5 \times 10^{-15} \text{ erg cm}^{-2} \text{ s}^{-1}$ in the direction of the *Lockman Hole* ($\text{RA} = 10^{\text{h}} 52^{\text{m}} 00^{\text{s}}$, $\delta = 57^{\circ} 21' 36''$). Following Maoz and Grindlay 1995, we first evaluate the distance r_* from Earth at which a DC with luminosity \mathcal{L}_X^{DC} yields a flux of $2.5 \times 10^{-15} \text{ erg cm}^{-2} \text{ s}^{-1}$. We find $r_* \simeq 7 \times 10^{-2} (M_{DC}/M_{\odot})^{1/2} \text{ kpc}$. Next, we assume for simplicity that DCs are distributed according to the standard spherical halo model. Denoting by R the galactocentric distance of a DC, the DC number density $n_{DC}(R)$ is

$$n_{DC}(R) = n_0 \left(\frac{a^2 + R_0^2}{a^2 + R^2} \right), \quad (10)$$

with $n_0 \simeq 0.9 \times 10^{-2} (M_{\odot}/M_{DC}) \text{ pc}^{-3}$, the core radius $a \simeq 5 \text{ kpc}$ and our galactocentric distance $R_0 \simeq 8.5 \text{ kpc}$. For our purposes, we parametrize a generic point in the halo by galactic spherical coordinates (r, b, l) taking the Earth as the origin. Accordingly, the relation between r and R is $R(r) = (r^2 + R_0^2 - 2rR_0 \cos b \cos l)^{1/2}$. With eq. (10), by straightforward steps we obtain

$$\mathcal{N} \simeq 3 \times 10^{-4} n_0 \int_{r_1}^{r_*} dr r^2 \frac{a^2 + R_0^2}{a^2 + R(r)^2} \text{ deg}^{-2}, \quad (11)$$

where the integral is taken along the line of sight towards the *Lockman Hole* and $r_1 \simeq 2.5 \text{ kpc}$ (corresponding to $R \simeq 10 \text{ kpc}$). In Table 2 we report \mathcal{N} for different values of M_{DC} , along with the total number \mathcal{N}_T of DCs per square degree. As

it can be seen $\mathcal{N} \sim 20 \text{ deg}^{-2}$ (for $M_{DC} \sim 10^5 M_\odot$) and thus the DCs can explain at most $\sim 20\%$ of the new population of faint X-ray sources.

Table 2. The number \mathcal{N} of faint X-ray sources per square degree towards the *Lockman Hole* with flux larger than $2.5 \times 10^{-15} \text{ erg cm}^{-2} \text{ s}^{-1}$ is shown in column 3 for some values of M_{DC} , assuming $L_X^M \sim 10^{27} \text{ erg s}^{-1}$. The last column gives the total number of DCs \mathcal{N}_T per square degree, irrespective of their flux (here we assume an amount of galactic dark matter of $\sim 10^{12} M_\odot$).

| $M_{DC} (M_\odot)$ | $n_0 (\text{pc}^{-3})$ | \mathcal{N} | \mathcal{N}_T |
|--------------------|------------------------|---------------|-------------------|
| 10^3 | 9.3×10^{-6} | – | 2.6×10^4 |
| 10^4 | 9.3×10^{-7} | 18 | 2.6×10^3 |
| 10^5 | 9.3×10^{-8} | 21 | 2.5×10^2 |
| 10^6 | 9.3×10^{-9} | 12 | 2.6×10^1 |

Finally, two points have to be mentioned. First, the $\log N - \log S$ diagram (see Fig. 8 in Hasinger et al. 1993) shows a moderate deficit of sources below a few $10^{-15} \text{ erg cm}^{-2} \text{ s}^{-1}$ (which is roughly the flux expected from DCs of mass $\sim 10^5 M_\odot$ at a distance larger than $\sim 10 - 20 \text{ kpc}$) with respect to the $-3/2$ behaviour (homogeneous distribution of X-ray sources). This fact can be naturally accounted for within the present model, since the source number density $n_{DC}(R)$ decreases as R^{-2} at large distance, implying a flattening in the $\log N - \log S$ diagram from $-3/2$ to $-1/2$. However, it is difficult to disentangle the individual contributions from objects with a different distribution in space (see Fig. 4 in Hasinger 1996 and Fig. 6 in McHardy et al. 1997). Second, the average spectrum of the faint sources gets harder ($HR \rightarrow 1$) at the lowest limiting flux (see Fig. 3 in Hasinger et al. 1993). Also this fact can be explained within our model, since absorption (from molecular gas in DCs) reduces the X-ray flux on Earth and increases HR .

3.3. Dark clusters and the diffuse XRB

Let us estimate the contribution of DCs to the diffuse XRB – namely the case for the DCs corresponding to region *C* of Fig. 1. The expected X-ray flux per unit solid angle in the direction (b, l) is given by (in $\text{erg cm}^{-2} \text{ s}^{-1} \text{ sr}^{-1}$)

$$\Phi_X(\nu_1, \nu_2; b, l) = \int_{r_{\min}(b, l)}^{r_{\max}(b, l)} dr n_{DC}(R(r)) \frac{\mathcal{L}_X^{DC}(\nu_1, \nu_2)}{4\pi}. \quad (12)$$

The best chance to detect the X-rays in question is provided by observations at high galactic latitude (or towards the *Lockman Hole*) and thus we evaluate $\Phi_X(\nu_1, \nu_2; 90^\circ)$. Therefore, we can safely take $r_{\min} \simeq 10 \text{ kpc}$ and $r_{\max} \simeq 100 \text{ kpc}$. The resulting X-ray fluxes are plotted in Figs. 2a - 2c (for different energy bands) as a function of T and for various galactic models. For each band, the horizontal line shows, for comparison, the diffuse unresolved XRB excess (with respect to the resolved discrete source contribution). As we can see, the DC emission can at most account for a few percents of the observed XRB flux. A somewhat higher flux has been obtained by Kashyap et al. 1994 for an unclustered population of MACHOs.

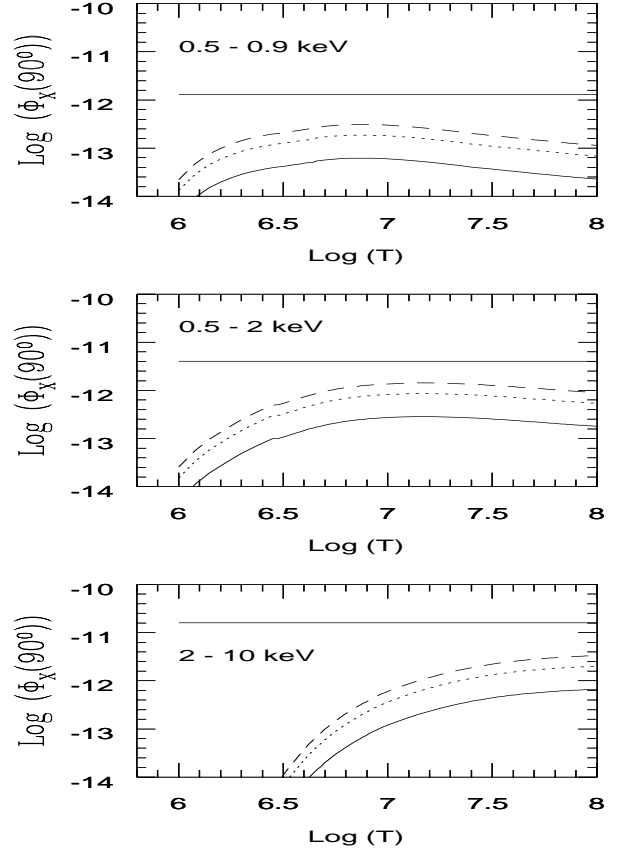


Fig. 2. The X-ray flux $\Phi_X(90^\circ)$ (in units of $\text{erg s}^{-1} \text{ cm}^{-2} \text{ deg}^{-2}$) at high galactic latitude due to the DC emission - see eq. (12) - is given, in various bands, as a function of the MACHO temperature T in K. To be definite we choose $L_X^M \sim 10^{27} \text{ erg s}^{-1}$, $f \sim 0.5$ and an intermediate value for g (see Table 1). We consider three different values for the total galactic dark matter M_{gal} : the full lines are for $M_{\text{gal}} = 1 \times 10^{12} M_\odot$, the dotted lines for $M_{\text{gal}} = 3 \times 10^{12} M_\odot$ and the dashed lines for $M_{\text{gal}} = 5 \times 10^{12} M_\odot$. For comparison, we show the corresponding XRB values in the various energy bands: 1.3×10^{-12} , 4×10^{-12} , $1.6 \times 10^{-11} \text{ erg cm}^{-2} \text{ s}^{-1} \text{ deg}^{-2}$, respectively.

4. Limits on the Amount of Virialized Diffuse Gas

One of the most intriguing recent results in the study of the diffuse XRB has been the detection by ROSAT of shadows in the $1/4 \text{ keV}$ XRB $0.15 - 0.28 \text{ keV}$ towards high-latitude interstellar clouds in Draco (Burrows and Mendenhall 1991, Snowden et al. 1991). Data show that about one half of the emission originates beyond these clouds and this fact is consistent with the presence of a $T \sim 10^6 \text{ K}$ diffuse halo gas in our galaxy³. Below, we are going to derive an upper bound on the amount of this virialized diffuse halo gas by fully tracing back to it the whole XRB excess in the $0.5 - 2 \text{ keV}$ band. Assuming that a fraction η of the galactic halo dark matter is in the form of virialized diffuse gas and that this is distributed like the dark

³Other spirals are observed to have diffuse X-ray halos as a consequence of the presence of hot diffuse gas, heated by the galactic gravitational field at virial temperatures $\sim 10^6 \text{ K}$ (Cui et al. 1996). The inferred typical X-ray luminosities are $\sim 10^{39} - 10^{40} \text{ erg s}^{-1}$, substantially less than that of bright ellipticals.

matter (namely according to eq. (10)), the X-ray flux on Earth (in units of $\text{erg cm}^{-2} \text{s}^{-1} \text{sr}^{-1}$) is

$$\Phi_X^{\text{gas}}(b, l) = \frac{\eta^2}{4\pi} \left(\frac{\rho_0}{\mu m_H} \right)^2 I_1(b, l) I_X(T, Z, b, l), \quad (13)$$

where $\mu \sim 1.22$ is mean molecular weight of the ionized gas, $\rho_0 \simeq 0.015 M_\odot \text{pc}^{-3}$ is the local dark matter density, while $I_1(b, l)$ and $I_X(T, Z, b, l)$ are as follows

$$I_1(b, l) = \int_0^{r_{\text{max}}} dr \left(\frac{a^2 + R_0^2}{a^2 + R(r)^2} \right)^2, \quad (14)$$

$$I_X(T, Z, b, l) = \int_{\nu_1}^{\nu_2} d\nu f(\nu, T, Z) e^{-\tau_{\text{disk}}(\nu, b, l)}, \quad (15)$$

where $f(\nu, T, Z)$ is defined via ϵ_ν and $\tau_{\text{disk}}(\nu, b, l)$ denotes the optical depth of the disk. Table 3 gives η as a function of T for several values of Z . As we can see, no more than 5% of the matter in the halo of our galaxy can be in the form of virialized diffuse gas. This conclusion makes the possibility of an *unclustered* MACHO population in the galactic halo unpalatable, since then the leftover gas would remain diffuse within the halo and should be virialized today.

Table 3. The upper limit on the fraction η of halo dark matter in the form of diffuse gas is given for some values of the gas temperature T (close to the virial temperature $1.6 \times 10^6 \text{ K}$) and for some values (arbitrarily selected) of gas metallicity Z . The fraction η is evaluated by means of eq. (13) assuming that the whole XRB excess at high galactic latitude is due to the diffuse gas emission. We consider a total mass and radius of the Galaxy $\sim 1.1 \times 10^{12} M_\odot$ and $\sim 120 \text{ kpc}$, respectively.

| $T \text{ (K)} =$ | 1.2×10^6 | 1.6×10^6 | 2.0×10^6 |
|-----------------------|-------------------|-------------------|-------------------|
| $Z = 10^{-3} Z_\odot$ | 5.2 | 3.3 | 2.5 |
| $Z = 10^{-2} Z_\odot$ | 4.9 | 3.1 | 2.4 |
| $Z = 10^{-1} Z_\odot$ | 3.1 | 2.0 | 1.6 |
| $Z = 1 Z_\odot$ | 1.2 | 0.8 | 0.6 |

5. Discussion and conclusions

The possibility that MACHOs with mass $\sim 0.1 M_\odot$ possess, in analogy with low-mass stars, coronal X-ray emission has several observational consequences. Indeed, according to the considered model for the halo dark matter, the large number of MACHOs inside each DC gives rise to a total X-ray luminosity \mathcal{L}_X^{DC} as high as $10^{29} - 10^{32} \text{ erg s}^{-1}$, in spite of the strong absorption brought about by molecular clouds.

The main parameter discriminating between different values of \mathcal{L}_X^{DC} is M_{DC} (see Fig. 1), which lies in the broad range $3 \times 10^2 - 10^6 M_\odot$. At the lower end of this range, namely for $M_{DC} \lesssim 10^4 M_\odot$, DCs can contribute to the XRB at a level of at most 5%. Of course, the latter value depends on the assumed total amount of halo dark matter, the coronal MACHO temperature and the considered energy range. For $M_{DC} \sim 10^5 M_\odot$ we get a different observational situation. In this case, fluctuation analyses of the XRB should yield ~ 20 DCs per square degree with X-ray flux in the range $2.5 \times 10^{-15} - 10^{-13} \text{ erg}$

$\text{cm}^{-2} \text{s}^{-1}$. This conclusion supports the idea that DCs contribute to the new population of faint X-ray sources advocated by Hasinger et al. 1993, 1996 and McHardy et al. 1997. Finally, if $M_{DC} \sim 10^6 M_\odot$, some DCs should be observable as resolved sources with the future planned satellite missions. The best strategy would then be to look in the direction of a previously microlensed star towards the LMC.

We have also derived an upper limit on the amount of virialized diffuse halo gas by using ROSAT data. Even if dependent on the gas virial temperature (and thus on the total dynamical mass of the Galaxy) and on the metallicity, this limit shows that the amount of diffuse gas in the galactic halo is less than 5%. This result corroborates our assumption that the primordial gas left over from MACHO formation should remain within the DCs (in the form of cold molecular clouds), for otherwise it would be heated by the gravitational field thereby emitting in the X-ray band.

Acknowledgements. We would like to thank A. Fabian for useful discussions. FDP is partially supported by the *Dr. Tomalla Foundation*, GI by the *Agenzia Spaziale Italiana* and MR by the *Dipartimento di Fisica Nucleare e Teorica, Università di Pavia*.

References

- Alcock, C. et al. 1993, Nat 365, 621
- Aubourg, E. et al. 1993, Nat 365, 623
- Barbera, M. et al. 1993 ApJ 414, 846
- Burrows, D. N. & Mendenhall, J. A. 1991, Nat 351, 629
- Cui, W. et al. 1996, ApJ 468, 102
- De Paolis, F., Ingrosso, G., Jetzer, Ph. & Roncadelli, M. 1995, A&A 295, 567
- De Paolis, F., Ingrosso, G. & Jetzer, Ph. 1996, ApJ 470, 493
- De Paolis, F., Ingrosso, G., Jetzer, Ph. & Roncadelli, M. 1996a, Int. J. of Mod. Phys.D 5, 151
- De Paolis, F., Ingrosso, G., Jetzer, Ph. & Roncadelli, M. 1996b, preprint ZU-TH 8/96, submitted to ApJ
- Drake, J. J. et al. 1996, ApJ 469, 828
- Evans, N. W. 1996, astro-ph 9611161
- Fall, S. M. & Rees, M. J. 1985, ApJ 298, 18
- Fleming et al. 1993, ApJ 410, 387
- Gates E.J., Gyuk G. & Turner M., 1996, Phys. Rev., D53, 4138
- Gerhard O. & Silk J. 1996, ApJ 472, 34
- Hasinger, G et al. 1993, A&A 275, 1
- Hasinger, G. 1996, A&AS 120, 607
- Kashyap, V., Rosner, R., Schramm, D. & Truran, J. 1994, ApJ 431, L87
- Maoz, E & Grindlay, J. E. 1995, ApJ 444, 183
- McHardy, I. M. et al. 1997, astro-ph 9703163
- Morrison, R. & McCammon, D. 1983, ApJ 270, 119
- Mullan, D. J. & Fleming, T. A. 1996, ApJ 464, 890
- Nulsen P.E.J. & Fabian A.C., 1997, submitted
- Raymond, J. C. & Smith, B. W. 1977, ApJS 35, 419
- Schmitt, J. H. M. M. et al. 1990, ApJ 365, 704
- Snowden, S. L. et al. 1991, Science 252, 1529
- Zaritsky, D. et al. 1989, ApJ 345, 759